J. Physiol. (1987), **393**, *pp.* 73–89
With 6 text-figures
Printed in Great Britain

CELL AND LUMINAL ACTIVITIES OF CHLORIDE, POTASSIUM, SODIUM AND PROTONS IN THE LATE DISTAL TUBULE OF *NECTURUS* KIDNEY

BY TAKIS ANAGNOSTOPOULOS AND GABRIELLE PLANELLES*

From the INSERM U. 192 Renal Physiology Laboratory, Hôpital Necker-Enfants-Malades, Paris, France

(*Received 23 February 1987*)

SUMMARY

1. Double-barrelled (selective *vs.* conventional) microelectrodes were used to assess the steady-state activities (a) of the ions Cl^-, K^+, Na^+ and H^+ in peritubular blood capillaries (a_{bld}) and in cell (a_{cell}) and lumen (a_{lum}) of the late distal tubule (l.d.t.) of *Necturus*.

2. a^{Cl}_{cell}, a^{Cl}_{lum} and a^{Cl}_{bld} were $5{\cdot}5 \pm 0{\cdot}3$, $11{\cdot}8 \pm 1{\cdot}0$ and $70{\cdot}5 \pm 0{\cdot}1$ mM, respectively. They were used to compute the chemical potentials for Cl^- across the three diffusive barriers of the tissue. Basolateral and apical membrane potentials were $-74{\cdot}3 \pm 1{\cdot}1$ and $-60{\cdot}1 \pm 2{\cdot}0$ mV, respectively (cell negative); the lumen was thus negative with respect to blood, by $13{\cdot}6 \pm 1{\cdot}5$ mV. The electrochemical potential difference (e.p.d.) for Cl^- of 42 mV across the apical membrane opposes Cl^- absorption, implying active apical Cl^- uptake, since Cl^- is known to be absorbed in the l.d.t. Basolateral Cl^- exit is favoured by an e.p.d. of 10 mV.

3. a^{K}_{cell}, a^{K}_{lum} and a^{K}_{bld} were $65{\cdot}8 \pm 0{\cdot}8$, $2{\cdot}5 \pm 0{\cdot}1$ and $2{\cdot}5 \pm 0{\cdot}1$ mM, respectively. The electrochemical distribution of K^+ indicates that K^+ absorption, if present, proceeds against an adverse apical e.p.d. of 18 mV. Basolateral K^+ distribution is close to its electrochemical equilibrium, suggesting high K^+ permeability at this membrane.

4. a^{Na}_{cell} was $9{\cdot}0 \pm 0{\cdot}4$ mM, a^{Na}_{bld} $71{\cdot}0 \pm 0{\cdot}3$ mM, and a^{Na}_{lum} was approximated at about 9 mM. Diffusive Na^+ entry from lumen to cell is favoured by an e.p.d. close to 65 mV. Basolateral Na^+ exit must be active, since it proceeds against an e.p.d. of 130 mV.

5. Cell, luminal and blood pH were $7{\cdot}14 \pm 0{\cdot}03$, $6{\cdot}52 \pm 0{\cdot}08$ and $7{\cdot}37 \pm 0{\cdot}04$, respectively. The luminal electrochemical potential of H^+ is higher than that of cell (by 91 mV) and blood (by 34 mV) indicating that proton secretion into the lumen must be active.

6. The e.p.d. of each ion across the epithelium opposes, by its orientation, the established direction of net transepithelial ion transport, suggesting that the shunt pathway may serve only for back-diffusion.

* The authors' names are in alphabetical order.

INTRODUCTION

The amphibian distal nephron is made up of at least two distinct portions, early or diluting (e.d.t.) and late distal tubule (l.d.t.) (Stoner, 1977). The former has been the focus of intensive investigation and shown to share a number of functional characteristics with the thick ascending limb of Henle's loop of the mammalian nephron. By contrast, little attention has been paid to the l.d.t. Isolated fragments taken from its terminal portion and perfused *in vitro* have been shown to develop lumen-negative transepithelial potential differences (V_{TE}), of about -40 mV (Stoner, 1977). V_{TE} was somewhat lower *in vivo*, on average -6 mV (Hoshi, Suzuki & Itoi, 1981; Cohen, Giebisch, Hansen, Teuscher & Wiederholt, 1984) to -15 mV (Teulon & Anagnostopoulos, 1982*a*), though on occasion V_{TE} reached -35 mV in late portions of this segment (Teulon & Anagnostopoulos, 1982*a*). Initial determinations of intraluminal ion concentrations along the distal tubule of *Necturus in vivo* revealed a substantial axial decline of luminal Na^+ and Cl^- concentrations, consistent with the observed net NaCl absorption along this segment (Bott, 1962); subsequent work confirmed the decrease of Na^+ concentration (Wiederholt, Sullivan & Giebisch, 1971; Garland, Henderson & Brown, 1975; Persson & Persson, 1983) and of total electrolyte concentration (Hoshi *et al.* 1981) along the amphibian distal tubule. Tubule to plasma K^+ concentration ratio showed variability, but it was essentially lower than 1·00 in the second half of the distal tubule of *Necturus* (Bott, 1962); this ratio was found to decline from $\sim 1{\cdot}50$ to $\sim 0{\cdot}80$ along the distal tubule of *Amphiuma*, (Wiederholt *et al.* 1971) or display a large scatter and remain close to 1·00 in the second half of this segment in *Necturus* (Garland *et al.* 1975). The pH of luminal fluid has been reported to decrease along the distal tubule of *Amphiuma* (Persson & Persson, 1983).

Since water is absorbed in the amphibian distal tubule (Bott, 1962; Wiederholt *et al.* 1971; Garland *et al.* 1975), the decrease of luminal Na^+ and Cl^- concentrations longitudinally indicates that they are reabsorbed in this segment, including its late portion. K^+ is normally absorbed in the l.d.t., but secretion is also possible under certain conditions (Wiederholt *et al.* 1971). However, such studies do not provide information about the site (membrane) of the active step generating net ion transport. To obtain this information, the orientation of the electrochemical driving forces across each barrier of the epithelium must be determined.

The purpose of the present work was to define the electrochemical potential differences of the ions Cl^-, K^+, Na^+ and H^+ across the basolateral and apical cell membranes and paracellular pathway of the l.d.t. of *Necturus in vivo*. We used double-barrelled microelectrodes to assess the activities of these ions in luminal fluid, cell and blood and to determine V_{TE} and cell membrane potential with regard to peritubular space (V_{BL}) and lumen (V_{AP}). In this way, the electrical, chemical and electrochemical potential differences of the main ions were determined across each barrier of the epithelium.

METHODS

The animals were kept in tap water at room temperature and fed twice a week. Urethane (15 g/l) was used to induce anaesthesia (by immersion) and was maintained by a dose of 3 g/l. The methods of preparing the kidney of *Necturus* and basic electrophysiological procedures have been

described in detail elsewhere (Anagnostopoulos, 1973; Edelman, Bouthier & Anagnostopoulos, 1981; Teulon & Anagnostopoulos, 1982*b*). The renal surface was continuously superfused with a Ringer solution in which electrolyte concentrations (mM) were: NaCl, 82; KCl, 3; $CaCl_2$, 1·8; $MgCl_2$, 1. The buffer was *N*-tris-(hydroxymethyl)methyl-2-amino-ethane sulphonic acid, 5 mM, and final pH was 7·4–7·6.

Identification of late distal tubules. In a previous study in *Triturus* kidney we found e.d.t.s to be located medially with regard to the glomeruli, and to have a small internal diameter ($\sim 40\ \mu m$) and lumen-positive potential, whereas l.d.t.s were lateral to the glomeruli and translucent, their diameter was intermediate to that of proximal and early distal tubules, and V_{TE} was lumen negative (Teulon & Anagnostopoulos, 1982*a*). The same optical criteria proved correct in 33 out of 35 pilot punctures in the present work, as judged from the values of V_{TE} and cast microdissections. The two erroneous choices were a straight proximal and an early distal tubule, as shown by their V_{TE} of 0 and +7 mV, respectively, and later confirmed by microdissection. In subsequent experiments, l.t.d.s were selected according to their morphology, with the condition that V_{TE} be more negative than −5 mV; when V_{TE} was between −5 and 0 mV, l.d.t. validation was achieved by oil injection via the glomerulus (Planelles, Moreau & Anagnostopoulos, 1983): the oil fills medial e.d.t. convolutions, then passes near the glomerulus, before reaching the l.d.t.

Construction of double-barrelled (selective vs. conventional) microelectrodes. The general procedures have been described in detail elsewhere (Teulon & Anagnostopoulos, 1982*b*). Aluminosilicate (o.d. 1 mm, i.d. 0·5 mm) or borosilicate (o.d. 1·2 mm, i.d. 0·7 mm) glass (Clark electromedical Instruments, U.K.) was used indifferently for making Cl^-, Na^+ and K^+ electrodes; borosilicate glass was used for pH-sensing electrodes. The selective barrel was exposed to vapours of dimethyl-trimethylsilylamine (Fluka 41720); Cl^- electrodes were occasionally exposed to hexamethyldisilazan (Fluka 52619). Ion-selective ligands were Corning 477913 (Cl^-), Corning 477317 (K^+), Fluka sodium-cocktail 71176 (Na^+) and Fluka proton-cocktail 82500 (H^+). Back-filling solutions were: NaCl, 100 mM, for Cl^- and Na^+ electrodes; KCl, 100 mM, for K^+ electrodes; NaCl, 67 mM + KH_2PO_4–K_2HPO_4, 33 mM, pH 7·00, for H^+ electrodes. The non-selective barrel contained 1 M-KCl or 1 M-sodium formate + 10 mM-NaCl (Cl^- electrodes); 1 M-KCl (Na^+, K^+ and H^+ electrodes). When necessary, the tip was gently bevelled in an alumina-powder suspension. The reference electrode was an Ag–AgCl junction connected via a 1 M-KCl agar bridge to the peritoneal cavity. Ion activities (a) were measured with an ultra-high-impedance electrometer (FD 223, WPI, New Haven, CT, U.S.A.); its output was displayed on a chart recorder (Sefram, Enertec-Schlumberger, France).

Cl^--selective electrodes. Calibration of these electrodes *in vitro*, between a reference solution in which NaCl concentration, [NaCl], was 82 mM (a^{Cl} = 65 mM) and pure NaCl solutions in which a^{Cl} was 12·4, 9 or 4·6 mM, yielded decade slopes of 55·6, 54·0 and 53·1 mV, respectively (Fig. 1, left). Addition of sodium gluconate (NaG) to a total [Na^+] of 82 mM resulted in lower slopes, 50·5 mV/decade in the a^{Cl} interval 65–11 mM, 47·5 mV/decade in the a^{Cl} interval 65–3·9 mM (Fig. 1, left). Gluconate in these solutions was assumed to represent, *in vitro*, the interference arising *in vivo* from the presence of intracellular organic anions; this interference is rather small in proximal tubular cells (Spring & Kimura, 1978).

Since the *in vitro* calibration was performed 2–4 h before the experiment and since repetitive tissue impalement may alter some electrode properties, tissue Cl^- activities were assessed *in vivo* as follows. The signal (differential output) issued upon cell impalement (a^{Cl}_{cell}), was compared to those obtained by placing the microelectrode tip in two test solutions, briefly flowing in succession onto the exposed peritoneal cavity: (i) 14 mM [NaCl] + 68 mM [NaG], (ii) 5 mM [NaCl] + 77 mM [NaG]. Similarly, the signal providing luminal Cl^- activity (a^{Cl}_{lum}), was referred to pure Cl^- solutions, 8 mM [NaCl] + 3 mM [KCl] and 14 mM [NaCl] + 3 mM [KCl], before or after impalement. In this way (i) the selectivity of the electrode was periodically checked, (ii) small changes in slope with time were taken into account, and (iii) when tip potentials occurred in dilute calibrating solutions, their value was subtracted from the corresponding differential signal. Our estimates of $[HCO_3^-]_{cell}$ and $[HCO_3^-]_{lum}$ were $\sim$ 2 and 1 mM, respectively (see below). Addition of $NaHCO_3$, 2 mM, to the 5 mM [NaCl] + 77 mM [NaG] calibrating solution or $NaHCO_3$, 1 mM, to the 11 mM [NaCl] + 3 mM [KCl] solution did not significantly affect the a^{Cl} signal.

K^+-selective electrodes. K^+ electrodes were calibrated *in vitro* as described above for Cl^- electrodes. K^+ concentration (activity) in pure KCl test solutions was 70 (59), 10 (9), 3 (2·8) and 2 (1·9) mM. The average slope between the reference 70 (59) mM-KCl and solution and solutions of stepwise decreased K^+ was 55·9, 51·8 and 49·2 mV/decade, respectively (Fig. 1, middle). Addition of NaCl,

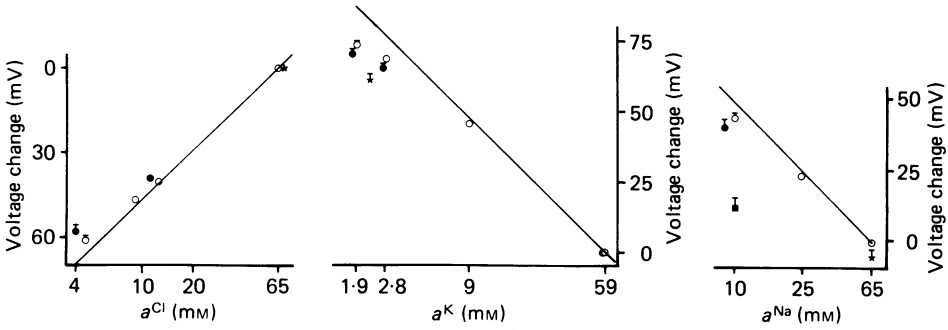

Fig. 1. Calibration procedures. The left panel shows *in vitro* calibration of the nine Cl^--selective electrodes used for impalements. Voltage change (selective channel output) is plotted as a function of a^{Cl}. Reference is a pure NaCl solution in which Cl^- concentration (activity) was 82(65) mM. Continuous line represents a slope of 58 mV per decade. [NaCl] (a^{Cl}) in other pure NaCl solutions (○) were 14 (12·4), 10 (9) or 5 (4·6) mM. Appropriate activity coefficients, γ, were used to convert concentrations to activities (Robinson & Stokes, 1959). In mixed solutions (●), sodium gluconate (NaG) was added to a total [Na^+] of 82 mM, to yield [Cl^-] (a^{Cl}) values of 14 (11) and 5 (3·9) mM. γ_G was assumed similar to γ_{Cl}, as are γ values of several monovalent organic anions of molecular weights comparable to that of gluconate (Robinson & Stokes, 1959, p. 493). Note that the value of [Cl^-] = 14 mM yields two different a^{Cl} values, depending on ionic strength, and so does [Cl^-] = 5 mM. It is also aparent that addition of gluconate results in a decrease in electrode slope. The selectivity coefficient $k_{Cl/G}$ was computed between a pure 82 mM [NaCl] solution and a 5 mM [NaCl] + 77 mM [NaG] solution, according to:

$$k_{Cl/G} = a^{Cl}_{pu} \times 190^{(V_{mix}-V_{pu})/S}/a^{G}_{mix},$$

where subscripts pu and mix refer to pure and mixed solutions, $V_{mix} - V_{pu}$ is the difference in potential between these solutions and S the slope in pure solutions. $k_{Cl/G}$ was thus estimated to be 0·02. Asterisk (*) corresponds to the Ringer solution. Vertical bars represent S.E.M., when larger than the size of symbol. The middle panel shows *in vitro* calibration of the six K^+-selective electrodes used for impalement. Mixed solution (●) contain 11 mM [NaCl] + 0·8 mM [$CaCl_2$] in addition to K^+. Conversion from [K^+] to a^K was obtained from appropriate γ_K at each [K^+] (Robinson & Stokes, 1959). The $k_{K/Na}$ coefficient, computed as above for $k_{Cl/G}$, was 0·025 between a pure high-K^+ solution (a^K = 59 mM) and a Ringer solution (a^K = 2·3, a^{Na} = 65 mM). It increased to ~ 0·08 in low-K^+ solutions (a^K = 1·8–2·7 mM), pure *vs.* supplemented with 11 mM-NaCl, indicating reduced selectivity of the exchanger in dilute mixed solutions. Addition of $CaCl_2$, 0·8 mM, to these solutions did not produce additional shift in potential difference. The right panel shows *in vitro* calibration of the six Na^+-selective electrodes used in this study. [NaCl] (a^{Na}) in pure solution was 82 (65), 30 (25·4) or 11 (10) mM. The 11 mM [NaCl] solution was supplemented with either KCl, 75 mM (●), or $CaCl_2$, 0·8 mM (■). The average slope in pure NaCl solutions was 55·1 mV/decade (a^{Na} interval 65–25·4 mM) or 52·5 mV/decade (a^{Na} 65–8·6 mM). Addition of KCl, 75 mM, to the low-Na^+ solution resulted in a +3·5 mV shift reflecting some interference of K^+ ions with the Na^+ ligand. $k_{Na/K}$ in 11 mM [NaCl] solutions, pure *vs.* supplemented with KCl, 75 mM, was 0·05. Addition of $CaCl_2$, 0·8 mM, into a 11 mM [NaCl] solution resulted in a large interference (+32 mV). Even small amounts of Ca^{2+}, 1·8 mM, added to the 82 mM [NaCl] solution (Ringer solution) produced an appreciable change in potential difference, 5·5 mV, indicating that the Na^+ liquid ion exchanger is more sensitive to Ca^{2+} than to Na^+.

15 mM, to the 70 mM [KCl] solution (to assess possible interference from intracellular Na^+ during a^K_{cell} determinations) did not alter the baseline electrical signal (Fig. 1, middle). By contrast addition of NaCl, 11 mM, and $CaCl_2$, 0·8 mM, to either the 3 mM [KCl] solution (a^K = 2·7) or the 2 mM [KCl] solution (a^K = 1·8 mM) resulted in an approximately +3 mV shift in potential difference (Fig. 1, middle); Na^+, not Ca^{2+}, was responsible for this shift (not shown). Such changes in potential

difference correspond to lower slopes, 49 mV/decade between 59 and 2·7 mM a^K, 46·3 mV/decade in the 59–1·8 mM a^K interval. However, the electrode slope in low-K^+ solutions (a^K 1·8–2·7 mM) supplemented with 11 mM-NaCl + 0·8 mM-$CaCl_2$ (these solutions are assumed to mimic l.d.t. luminal fluid), was only 25·2 mV/decade. Obviously, a^K_{lum} cannot be assessed with good precision in this range.

K^+ activities *in vivo* were obtained by comparing the differential signal during cell or luminal impalement to that in pertinent artificial solutions briefly flowing onto the exposed peritoneal cavity: (i) the intracellular K^+ reading was referred to that of a 75 mM [KCl] + 15 mM [NaCl] solution (a^K = 58 mM) and converted to a^K_{cell} using the appropriate slope established *in vitro*. (ii) Luminal K^+ determinations were obtained by graphed calibration against mixed solutions containing [KCl] of 2, 3 or 5 mM, and in all cases 11 mM [NaCl] + 0·8 mM [$CaCl_2$].

Na^+-selective electrodes. Calibration of Na^+ electrodes was performed *in vitro*, first in pure NaCl solutions, then in solutions containing high amounts of KCl (to assess possible distortion produced by K^+ ions in the intracellular compartment), or in solutions supplemented with millimolar concentrations of $CaCl_2$, comparable to those prevailing in extracellular fluid. Results are summarized in Fig. 1, right.

There are two main observations. (i) The high intracellular K^+ produces a small but significant interference with the Na^+ signal, which must be taken into account in the calculation of a^{Na}_{cell}. By contrast, addition of KCl, 3 mM, into a pure 82 mM [NaCl] solution did not alter the a^{Na} signal (not shown). (ii) The Na^+ ligand is extremely sensitive to Ca^{2+} ions. Addition of $CaCl_2$, 0·8 mM, (the average Ca^{2+} concentration prevailing in late distal tubular fluid of *Necturus* (Garland *et al.* 1975)) to an 11 mM [NaCl] solution produces a major shift of the Na^+-electrode signal (Fig. 1, right). Similar observations were reported in a recent study (García-Díaz, Klemperer, Baxendale & Essig, 1986), in which it was also shown that the Ca^{2+} interference vanishes at pCa > 6. Since pCa in amphibian renal cells is close to 7 (Lee, Taylor & Windhager, 1980) it is inferred that a^{Na}_{cell}, but not a^{Na}_{lum}, may be safely assessed with Na^+-selective electrodes.

Figure 1 (right) shows in addition that the presence of $CaCl_2$, 1·8 mM, to the Ringer reference solution brings about an average +5·5 mV shift in the Na^+-electrode signal, which must also be taken into account in the determination of a^{Na}_{cell}. Thus, a^{Na}_{cell} was obtained by graphed calibration, before or after impalement, by referring the intracellular signal to two artificial solutions (8 mM [NaCl] + 75 mM [KCl] and 15 mM [NaCl] + 75 mM [KCl]), briefly allowed to flow onto the exposed peritoneal cavity, not to the Ringer solution baseline. a^{Na}_{lum} was not measured.

pH-selective electrodes. The construction of such electrodes, calibration procedures and tests for possible interference from other ions have been described in detail elsewhere (Planelles, Kurkdjian & Anagnostopoulos, 1984). Their slope in the present study ranged between 50 and 58 mV per pH unit change. pH_{cell} and pH_{lum} were referred to the pH of the surface fluid flowing solution. $[HCO_3^-]_{cell}$ and $[HCO_3^-]_{lum}$ were estimated from the respective pHs using the Henderson–Hasselbalch equation and appropriate values for pK_a (= 6·17) and CO_2 solubility coefficient, α_{CO_2} (0·043 at 22 °C), applicable to cold-blooded animals (Reeves, 1976; Nicol, Glass & Heisler, 1983). The use of this equation seems justified *a priori*, in view of the presence of carbonic anhydrase in amphibian distal tubular cell membranes (Riddenstråle, 1976).

RESULTS

Cl^--selective microelectrodes

Paired measurements in eighteen tubules revealed that the intraluminal Cl^- activity, a^{Cl}_{lum}, was higher than a^{Cl}_{cell} (an example is illustrated in Fig. 2): 11·8 ± 1·0 *vs.* 5·5 ± 0·3 mM, respectively (Table 1). From these values and from the average Cl^- activity in peritubular capillaries, a^{Cl}_{bld}, 70·5 ± 0·4 mM (n = 7 animals), the equilibrium potentials for Cl^- across the basolateral cell membrane (E^{Cl}_{BL}), apical membrane (E^{Cl}_{AP}) and the whole epithelium (E^{Cl}_{TE}) may be estimated at −65, −18 and −47 mV, respectively (Table 1). The corresponding electrical potential differences were V_{BL} = −74 mV, V_{AP} = −60 mV and V_{TE} = −14 mV. The net electrochemical driving force for passive (diffusional) transport of Cl^- is the algebraic sum $V - E^{Cl}$. At the basolateral cell membrane, $V_{BL} - E^{Cl}_{BL}$ was thus −9 mV. The orientation of this

electrochemical potential difference is favourable for passive Cl^- exit from cell to interstitium. At the apical cell membrane, $V_{AP}-E^{Cl}_{AP}$ was -42 mV, indicating that the intracellular Cl^- is above electrochemical equilibrium with respect to lumen, thus favouring diffusional back-diffusion of Cl^- from cell to lumen (Fig. 3 and Table 1).

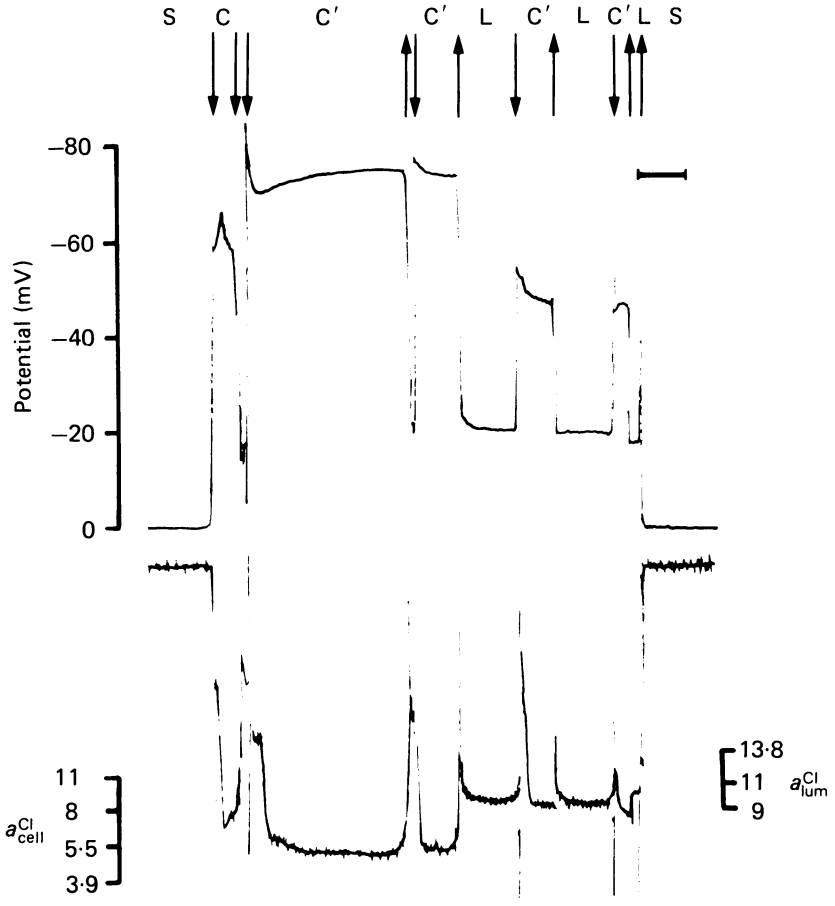

Fig. 2. Measurement of a^{Cl}_{cell} and a^{Cl}_{lum} in an l.d.t. C, C', L and S refer to tip positioning in a cell of the upper epithelial layer (C), a cell of the lower layer (C'), lumen (L) and surface fluid solution (S). Downward and upward arrows indicate advancement or withdrawal of the microelectrode, respectively. Time scale, 1 min. Top: electrical potential (scale in millivolts). Bottom: differential output ($V-E_{Cl}$); left-hand side scale, a^{Cl}_{cell}, right-hand side scale, a^{Cl}_{lum}. It is seen that only in two out of the five cellular impalements (second and third) was V_{BL} sufficiently stable to provide reliable a^{Cl}_{cell} estimates. When these values differed in a given tubule, their average was considered as a single measurement.

The transepithelial electrochemical potential difference, $V_{TE}-E^{Cl}_{TE}$, was $+33$ mV, directed from blood to lumen. Thus, the shunt pathway is unfavourable for Cl^- absorption; it could be a route of Cl^- back-diffusion if the shunt is permeable to Cl^-.

TABLE 1. Ion activities, chemical, electrical and electrochemical potential differences across the diffusive barriers of the l.d.t. of *Necturus in vivo*

	Activities			Basolateral			Apical			Transepithelial			
	Cell (mM)	Lumen (mM)	Blood (mM)	E_{BL} (mV)	V_{BL} (mV)	$V_{BL}-E_{BL}$ (mV)	E_{AP} (mV)	V_{AP} (mV)	$V_{AP}-E_{AP}$ (mV)	E_{TE} (mV)	V_{TE} (mV)	$V_{TE}-E_{TE}$ (mV)	N (n)
Cl^-	5·5±0·3	11·8±1·0	70·5±0·1	−64·8±1·1	−74·3±1·1	−9·5±1·7	−17·9±2·4	−60·1±2·0	−42·2±3·0	−46·9±2·5	−13·6±1·5	+33·3±2·8	18 (7)
K^+	65·8±0·8	2·47±0·10	2·51±0·07	−81·9±0·3	−78·1±0·8	+3·6±0·8	−83·1±0·9	−64·8±1·6	+18·3±1·6	+1·9±1·1	−12·4±1·5	−14·2±1·6	21 (5)
Na^+	9·0±0·4		71·0±0·3	+52·2±1·2	−77·3±1·2	−129·4±1·7		−65·0±2·0			−12·3±1·9		11 (5)
pH	7·14±0·03	6·52±0·08	7·37±0·04	−13·5±1·5	−70·5±1·7	−57·0±2·1	+36·2±3·8	−54·8±3·5	−90·9±5·6	−49·5±4·2	−15·8±2·9	+33·8±5·7	12 (5)
HCO_3^-	2·21±0·16	0·59±0·07	3·82±0·36	−13·5±1·5	−70·5±1·7	−57·0±2·1	+36·2±3·8	−54·8±3·5	−90·9±5·6	−49·5±4·2	−15·8±2·9	+33·8±5·7	
		(0·78±0·09)					(+29·0±3·7)		(−83·8±5·5)	(−42·3±4·1)		(+26·5±5·7)	

Paired measurements of a_{cell} and a_{lum} were always performed in single tubules. Values are expressed as means ± S.E.M. N (n) in each line indicates number of tubules (animals). [HCO_3^-] values were calculated from pH values according to the Henderson–Hasselbalch equation and, therefore, they do not constitute independent measurements; values in parentheses were obtained by raising individual pH_{lum} values by 0·12 units, to take into account the presence of an acid luminal disequilibrium pH (Persson & Persson, 1983).

K^+-selective microelectrodes

The mean intracellular K^+ activity was $65{\cdot}8 \pm 0{\cdot}8$ mM, substantially higher than luminal and peritubular capillary K^+ activities, both these values being estimated at 2·5 mM (Table 1). Figure 4 shows the measurement of a^{K}_{cell} and a^{K}_{lum} in an l.d.t.

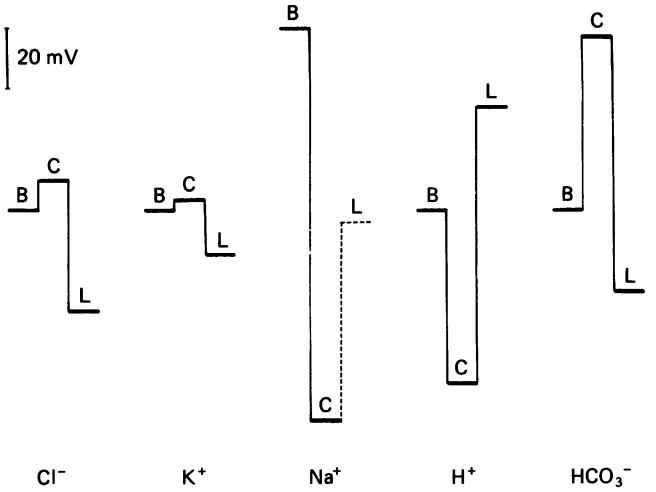

Fig. 3. Schematic representation of the average electrochemical potential differences for single ions, between blood (B), cell (C) and lumen (L). B is the reference. Levels above or below B (or with regard to each other), for a given species, indicate higher or lower electrochemical potentials, respectively. Interrupted line (Na^+) denotes calculated, not measured value. Luminal HCO_3^- concentration was corrected for an acid disequilibrium pH of 0·12 units.

Conversion of activity ratios to K^+ equilibrium potentials yielded the following values: $E^{K}_{BL} = -82$ mV, $E^{K}_{AP} = -83$ mV and $E^{K}_{TE} = +2$ mV. The corresponding electrical potential differences in the same tubules were $V_{BL} = -78$ mV, $V_{AP} = -65$ mV and $V_{TE} = -12$ mV (Table 1). The equilibrium potential for K^+ across the basolateral membrane is thus very close to V_{BL}, their difference $V_{BL} - E^{K}_{BL}$ being +3·6 mV. The chemical equilibrium potential for K^+ across the apical membrane (−83 mV) is higher than V_{AP} (−65 mV), giving (at least in the present series of experiments) an apical electrochemical driving force of +18 mV opposing K^+ absorption (Fig. 3). Similarly, the transepithelial electrochemical potential difference, of −14 mV, is oriented from blood to lumen, i.e. it favours K^+ secretion if the shunt pathway is permeant to K^+ (Fig. 3).

Na^+-selective microelectrodes

The mean intracellular Na^+ activity was $9{\cdot}0 \pm 0{\cdot}4$ mM (Table 1 and Fig. 5), a^{Na}_{bld}, was $71{\cdot}0 \pm 0{\cdot}3$ mM. The chemical Na^+ driving force for Na^+ across the basolateral cell membrane $E^{Na}_{BL} = +52$ mV, and the intracellular negativity of −77 mV yield an algebriac sum of −129 mV opposing Na^+ absorption (Fig. 3). That the steady-state a^{Na}_{cell} is very far from electrochemical equilibrium suggests very low Na^+ permeability at the basolateral cell membrane. Obviously, this distribution is the result of active Na^+ extrusion via the basolateral Na–K pump.

Attempts to assess a^{Na}_{lum} were unsuccessful (see Methods). Assuming that a^{Na}_{lum} may be approximated by the difference $a^{Cl}_{lum} - a^{K}_{lum} + [HCO_3^-]_{lum} - [Ca^{2+}]_{lum}$, i.e. ~ 9 mM, the electrochemical profile for Na^+ may be tentatively estimated across the apical membrane and shunt pathway. At the apical cell membrane, E^{Na}_{AP} is close to 0 mV

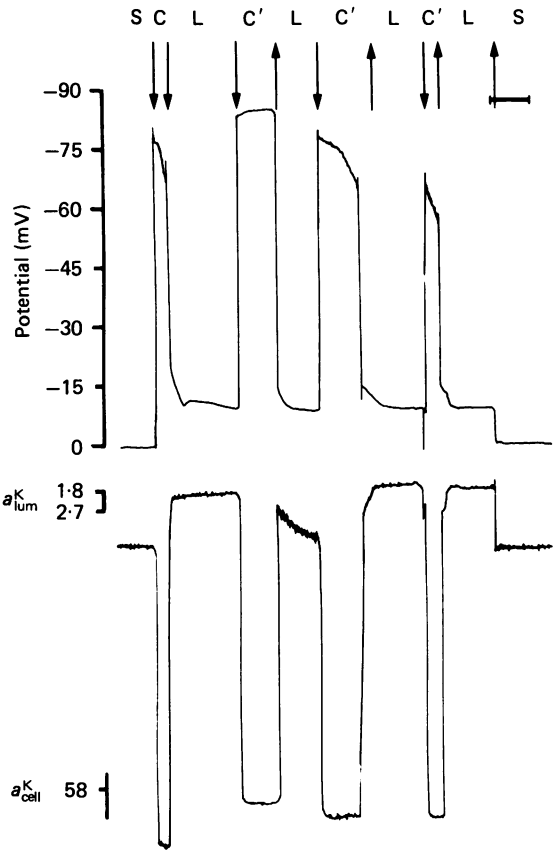

Fig. 4. Measurement of a^K_{cell} and a^K_{lum} in an l.d.t. Symbols and notation are as in Fig. 2. a^K_{lum} is compared to the signal of dilute solutions in which a^K was 1·8 and 2·7 mM; a^K_{cell} was referred to a solution containing 75 mM [KCl] + 15 mM [NaCl] (a^K = 58 mM). Two potential causes of error are illustrated in this recording. (i) Leaky cell impalements (first, third and fourth) tend to overestimate a^K_{cell}, simply because the fall of potential difference is proportionally larger than the concomitant decrease of a^K_{cell}, tending thus to increase the differential signal; therefore, only the second cell impalement of this tracing was taken into account for the calculation of a^K_{cell}. (ii) Occasionally, upon passage into the lumen after a cell impalement the differential signal is unexpectedly high and unstable. In such cases, impaling another cell and returning to the lumen often gives a lower, more stable signal. Such artifacts (second introduction into luminal fluid) are presumed to be due to debris on the tip which is dislodged by subsequent impalement.

(since $a^{Na}_{cell} \simeq a^{Na}_{lum}$), when $V_{AP} = -65$ mV. Therefore, a substantial electrochemical potential difference for Na^+, $V_{AP} - E^{Na}_{AP} \simeq -65$ mV, favours passive Na^+ entry from lumen to cell (Fig. 3). Only, if a^{Na}_{lum} were $< 0{\cdot}7$ mM, a highly unlikely hypothesis, would the net driving force for Na^+ reverse to produce Na^+ exit from cell to lumen. The transepithelial Na^+ distribution is defined by $V_{TE} = -12$ mV and by an equi-

librium potential E_{TE}^{Na} of approximately +52 mV, yielding a transepithelial electrochemical potential difference close to −64 mV, which favours paracellular Na^+ back-diffusion. Only for $a_{lum}^{Na} > 114$ mM would the direction of this driving force be inversed to contribute to Na^+ absorption, again a very unlikely contingency.

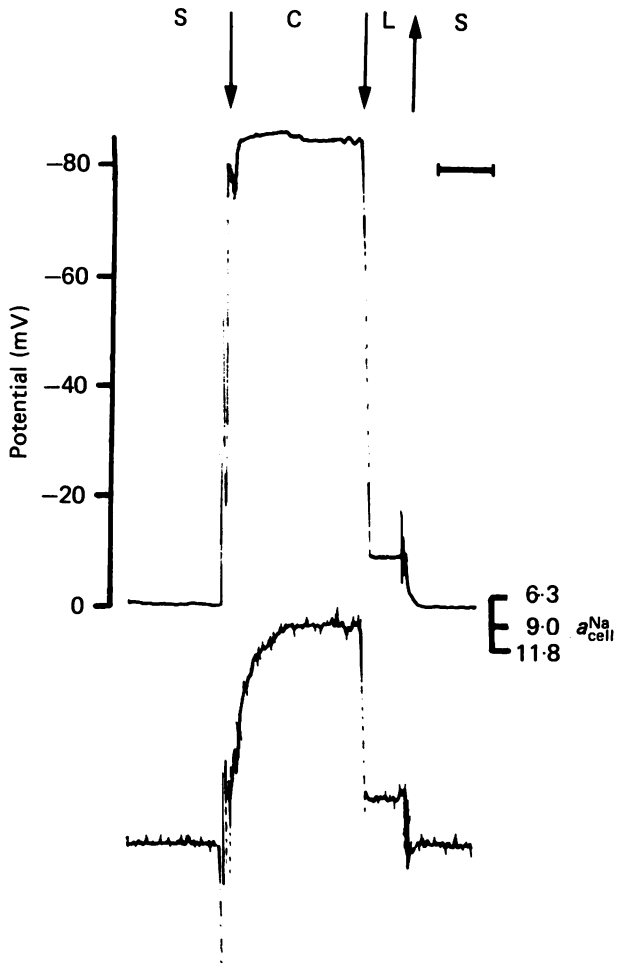

Fig. 5. Measurement of a_{cell}^{Na} with a Na^+-selective electrode. Symbols and notation as in Fig. 2. Right-hand-side scale refers to a^{Na} calibration *in situ*. Note the lumen negative V_{TE} (9 mV) and the huge interference from Ca^{2+} in luminal fluid.

pH-selective microelectrodes

The average values of pH_{cell} and pH_{lum}, in paired measurements, were 7·14 and 6·52, respectively; an example of such measurements is shown in Fig. 6. The value of pH_{bld} was 7·37 (Table 1). The intracellular negativity with regard to the blood side ($V_{BL} = -71$ mV) is quantitatively larger than the opposing basolateral H^+ chemical equilibrium potential of −14 mV (computed from pH_{cell} and pH_{bld}). Hence, the basolateral H^+ electrochemical potential difference, −57 mV, favours diffusional

entry of protons into the cell (Fig. 3). At the apical pole of the cell, the chemical driving force ($E^{H}_{AP} = +36$ mV) and the electrical potential ($V_{AP} = -55$ mV) both favour proton influx into the cell, giving net e.p.d. of -91 mV. Thus, the intracellular compartment behaves as a sink for protons at both poles of the cell

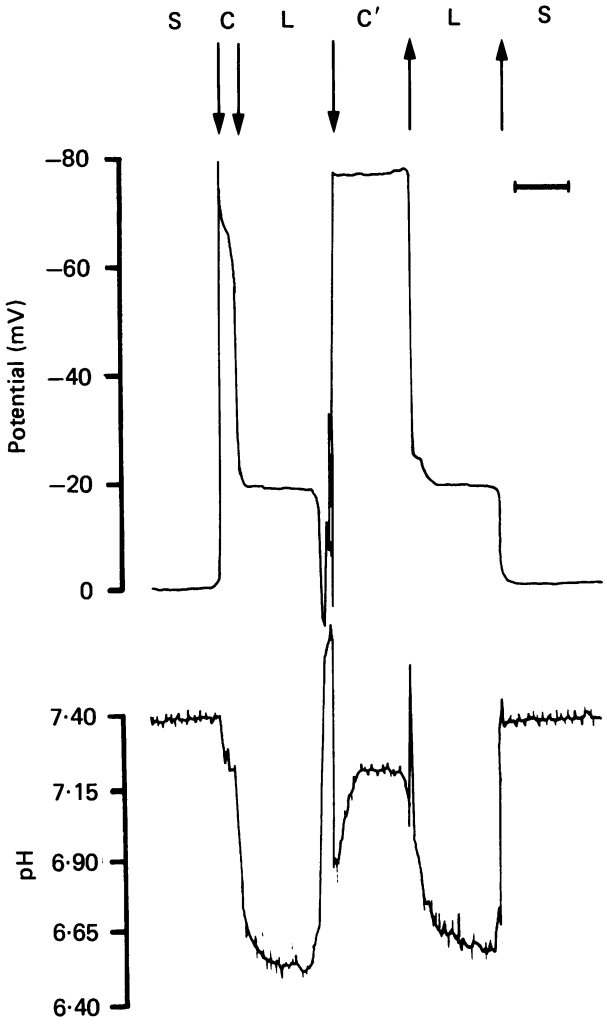

Fig. 6. Measurement of pH_{cell} and pH_{lum} in an l.d.t. Symbols and notation as in previous Figures.

(Fig. 3), implying the presence of active H^+ extrusion mechanisms at the apical or at both cell membranes. The transepithelial chemical driving force (-50 mV) is directed from lumen to blood and is larger than the opposing electrical potential difference (-16 mV), thus their net effect favours paracellular H^+ absorption. Taken together, these observations indicate active extrusion of protons (or equivalent species) from cell to lumen, i.e. across the apical cell membrane, generating an intraluminal H^+ electrochemical potential higher than those of cell and blood (Fig. 3).

From the measured pH values, the following tentative HCO_3^- concentrations may be estimated: $[HCO_3^-]_{bld}$ = 3·82 mM, $[HCO_3^-]_{cell}$ = 2·21 mM, $[HCO_3^-]_{lum}$ = 0·59 mM. Given the assumption of chemical equilibrium (Henderson–Hasselbalch) the resulting HCO_3^- equilibrium potentials should be identical to the corresponding H^+ equilibrium potentials. If, however, a luminal acid disequilibrium pH of 0·12 units prevails in the amphibian distal tubule (Persson & Persson, 1983), $[HCO_3^-]_{lum}$ should be raised from 0·59 to 0·78 mM; $E_{AP}^{HCO_3}$ and $E_{TE}^{HCO_3}$ should be corrected accordingly (Table 1). Such corrections do not affect the conclusions regarding possible mechanisms of HCO_3^- transport. At the basolateral cell membrane the e.p.d. $V_{BL} - E_{BL}^{HCO_3}$ (−57 mV) is appropriately oriented to favour diffusive HCO_3^- absorption. By contrast, at the apical cell membrane, both the chemical and electrical potential differences oppose HCO_3^- absorption, whether corrections for acid disequilibrium pH are made or not. Similarly, the paracellular pathway is, if anything, a route for HCO_3^- back-diffusion towards the luman (Fig. 3).

DISCUSSION

To our knowledge, this is the first report on transmembrane distribution of single ion species in the amphibian l.d.t. Since the present experiments deal with steady-state electrochemical profiles, not with dynamic responses to selected disturbances, they allow us to determine whether an ion is transported passively or actively (given the established direction of net transepithelial ion transport), but not to identify, in the latter case, the actual active mechanism(s). In the following we shall consider the relevance of some active transport systems, described or postulated in mammalian distal nephron, as possible mechanisms of uphill ion transport in the l.d.t. of *Necturus*, by taking into account the energetic constraints prevailing across each of its cell membranes.

Chloride

Cl^- has been shown to be absorbed along the entire length of the distal tubule (Bott, 1962). Since the transepithelial electrochemical potential difference for Cl^- favours paracellular back-diffusion, Cl^- absorption must be exclusively transcellular. At the apical cell membrane, absorptive transport of Cl^- must overcome an adverse energy barrier of some 42 mV (Fig. 3). Interestingly, an active step in Cl^- transport has also been reported across the apical rather than basolateral cell membrane in the 'late distal tubule' of the rat (Khuri, Agulian & Bogharian, 1974). At least three different mechanisms could account for uphill Cl^- transport at this site. (i) A primary Cl^- pump is a definite possibility, even though its occurrence is rare in the animal kingdom. Active electrogenic Cl^- absorption has been reported under certain circumstances in rabbit cortical collecting tubule (c.c.t.) (Hanley, Kokko, Gross & Jacobson, 1980), but its possible dependence on metabolic energy has not been investigated. (ii) An electroneutral anion antiporter exchanging Cl^- (from lumen to cell) against HCO_3^- (from cell to lumen) could account for cellular Cl^- uptake, since the chemical gradients of both Cl^- and HCO_3^- are favourably oriented for this exchange (Table 1). An apical anion exchanger has been suggested in the c.c.t. (Star, Burg & Knepper, 1985). It could be argued, however, against this hypothesis, that

Cl–HCO_3 exchange would tend to dissipate the proton gradient generated by active H^+ secretion into the lumen. (iii) An electroneutral Na–Cl symport. Both, Cl^- and Na^+ are absorbed in the amphibian distal tubule (Bott, 1962). The chemical gradient of Cl^- ($a^{Cl}_{lum}/a^{Cl}_{cell} = 2{\cdot}15$) favours its downhill entry into the cell, and therefore Cl^- entry could be coupled to that of Na^+, since a^{Na}_{lum} is very close to a^{Na}_{cell}. The limiting a^{Na}_{lum} value below which coupled Na–Cl entry should cease is 4·2 mM, given the measured a^{Na}_{lum} of 9 mM; NaCl absorption via this mechanism could be achieved even if a^{Na}_{lum} were lowered below 4·2 mM, if a^{Na}_{cell} decreased in parallel with a^{Na}_{lum} in l.d.t., as it does in frog skin epithelium (García-Díaz *et al.* 1986). Coupled Na–Cl (but not Na–K–2Cl) entry from lumen to cell has been reported in the rat distal convoluted tubule (Velázquez & Wright, 1986), a heterogeneous structure which, together with the c.c.t., are the best candidates of mammalian functional equivalent for the amphibian l.d.t. Na–K–2Cl or K–Cl symports are unlikely, for reasons discussed below.

At the basolateral cell membrane, Cl^- could exit the cell via a Cl^--conductive pathway, as described in rabbit c.c.t. (Sansom, Weinman & O'Neil, 1984). Without concomitant assessment of basolateral Cl^- permeability, it is not clear whether the favourable electrochemical potential difference of $\sim$ 10 mV is sufficient to account for downhill Cl^- absorption or whether additional transport mechanisms are also required. It is presenbly unknown whether the l.d.t. is a site of transepithelial Cl^- exchange–diffusion, as is the mammalian c.c.t. (Stoner, Burg & Orloff, 1974; Tago, Schuster & Stokes, 1986).

Sodium

In view of an adverse transepithelial e.p.d. in the absorptive direction, Na^+, like Cl^-, must be absorbed along the cellular route. The apical entry of Na^+ into the cell may be diffusive, along a favourable e.p.d. of about 65 mV, and/or coupled to Cl^-, as discussed above. The contribution of an apical electroneutral Na–H exchanger is highly unlikely in the present series of experiments: in the virtual absence of Na^+ concentration difference across the apical cell membrane, the average $[H^+]_{lum}/[H^+]_{cell}$ gradient of about 4·2 (computed from $pH_{lum} = 6{\cdot}52$ and $pH_{cell} = 7{\cdot}14$) would drive both species in the wrong direction, i.e. protons into the cell in exchange for Na^+ secreted into the lumen. Only at a^{Na}_{lum} values higher than 36 mM ($[Na^+] > 43$ mM), could Na^+ entry into the cell overcome the adverse chemical H^+ gradient and elicit coupled H^+ secretion into the lumen. However, the presence of a Na–H exchanger, ordinarily quiescent and possibly activated if pH_{cell} is lowered below pH_{lum}, cannot be ruled out.

Potassium

Na^+ and Cl^- are physiologically absorbed in the amphibian and in the mammalian distal nephron, whereas K^+ may be transported in either direction in both *Amphiuma* distal tubule (Wiederholt *et al.* 1971) and mammalian distal convoluted tubule, depending on metabolic and nutritional conditions. The present data probably pertain to the control state defined by Wiederholt *et al.* (1971), in which net K^+ absorption prevails. This conclusion stems from the observation that a^K_{lum}/a^K_{bld} in the terminal portion of the e.d.t. is $\sim$ 1·3 (Teulon, Froissart & Anagnostopoulos, 1985)

compared to our present average of 1·0 in l.d.t., despite the likely occurrence of water abstraction between these two sites. a^{K}_{lum}/a^{K}_{bld} ratios of 1·00 in *Amphiuma* distal tubule were observed only during K^+ absorption, by Wiederholt *et al.* (1971).

The observation that the transepithelial electrochemical potential difference for K^+ opposes K^+ absorption (it rather favours paracellular secretion) suggests that net K^+ absorption, if present, is transcellular. Since the apical cell membrane behaves as an electrochemical and a chemical energy barrier for K^+ absorption, it must carry an active transport step for K^+ absorption. The hypothesis of an electroneutral Na–K–2Cl symport is unlikely. The limiting a^{K}_{cell}/a^{K}_{lum} ratio that could be developed by this carrier is given by

$$a^{K}_{cell}/a^{K}_{lum} < (a^{Na}_{lum}/a^{Na}_{cell})\,(a^{Cl}_{lum}/a^{Cl}_{cell})^2.$$

The second term of this inequality barely attains a factor of 4·6 while a^{K}_{cell}/a^{K}_{lum} is close to 26. A neutral K–Cl symport is *a fortiori* ruled out since the activity of the driving ion ratio $a^{Cl}_{lum}/a^{Cl}_{cell} = 2{\cdot}15$, would have to be higher than the opposing a^{K}_{cell}/a^{K}_{lum} ratio of 26. A more plausible alternative for apical active K^+ uptake could be a K–H pump, similar to that reported in gastric mucosa (Sachs, Chang, Rabon, Schackmann, Lewin & Saccomani, 1976), rabbit distal colon (Halm & Frizzell, 1986) and *Amphiuma* jejunum (White, 1985). If this hypothesis is correct, uncoupling between the net fluxes of K^+ (entering from lumen to cell) and H^+ (secreted into the lumen), and related modulation of the net absorptive (or secretory) K^+ transport, could be achieved through a conductive K^+ pathway, in parallel to the postulated H–K pump, used for apical K^+ recycling.

At the basolateral cell membrane, Na–K pump-dependent K^+ uptake presumably contributes to the elevation of a^{K}_{cell} above electrochemical equilibrium. The nearly equal E^{K}_{BL} and V_{BL} suggest, but do not unequivocally prove, high basolateral permeability for K^+. A conductive K^+ pathway at this site, if present, could be used for (i) recycling K^+ ions actively transported into the cell via the Na–K pump, and (ii) for net K^+ absorption. The presence of distinct pump–leak K^+ mechanisms at both poles of the cell, if confirmed, could account for the ability of the l.d.t. to generate net K^+ absorption or net K^+ secretion (Wiederholt *et al.* 1971).

Protons

The observation of a luminal electrochemical potential for H^+ higher than those of cell and blood (Fig. 3) reflects the presence of an apically located active transport mechanism extruding H^+ (or equivalent species) into the lumen. It could be the neutral H–K pump mentioned above and/or an electrogenic apical H^+ pump, as described in the rabbit c.c.t. (Koeppen & Helman, 1982) and in bovine renal medulla (Gluck & Al-Awqati, 1984); a Na–H exchanger is unlikely, as already discussed. The observation that H^+ ions are not distributed at equilibrium across the basolateral cell membrane does not necessarily imply the presence of active extrusion of protons (or equivalent species) at this site too; an apical H^+ pump associated with low basolateral permeability to H^+ (and equivalent species) is consistent with the observed transepithelial electrochemical pattern. At least three other mechanisms may be implicated in the acid–base functions of the l.d.t. (i) A basolateral Na–H exchanger, subservient to pH_{cell} homeostasis, similar to that described in the mammalian c.c.t.

(Chaillet, Lopes & Boron, 1985); (ii) a basolateral $Cl–HCO_3$ exchanger, assigned to the disposal of excess intracellular base, generated by H^+ secretion. Although unambiguous demonstration of basolateral $Cl–HCO_3$ exchange is lacking in mammalian distal tubule and c.c.t., this exchanger is present in other tight epithelia, including the outer medullary collecting tubule (Stone, Seldin, Kokko & Jacobson, 1983), turtle bladder (Fischer, Husted & Steinmetz, 1983) and frog skin (Duranti, Ehrenfeld & Harvey, 1986); (iii) a basolateral HCO_3^- conductance contributing to HCO_3^- absorption. All these mechanisms, are energetically feasible. Their presence cannot be asserted without further experimental demonstration.

Conclusion

The present study establishes the chemical, electrical and electrochemical potential differences of the ions Cl^-, Na^+, K^+ and H^+ across the diffusive barriers of the l.d.t. in *Necturus*. The electrochemical gradients across the paracellular path for all of these ions are in the direction opposite to their established net transport, indicating major cellular routes for all of them. After elimination on energetic grounds of some *a priori* plausible alternatives, we retain the following as likely mechanisms of cellular transport. The active step for transcellular Cl^- transport appears to be at the apical cell membrane, and could be a primary Cl^- pump, a $Cl–HCO_3$ exchange or a Na–Cl symport; basolateral exit of Cl^- is, at least partly, diffusional. Na^+ enters from lumen to cell downhill, via Na–Cl symport and/or by simple diffusion; its basolateral exit is active, presumably dependent on the activity of the Na–K pump. When K^+ is absorbed, an active K^+ uptake step is necessary at the apical cell membrane; by elimination of other putative transport mechanisms a K–H pump appears as the most attractive possibility; basolateral exit is diffusive. Protons are actively secreted into the lumen either via the aforementioned K–H pump or by a primary H^+ pump, or both. Basolateral disposal of excess base equivalents could be achieved by HCO_3^- diffusion or by $Cl–HCO_3$ exchange.

This study was supported by C.N.R.S. GRECO 24. We acknowledge the expert technical assistance of Ph. Hulin and secretarial work of F. Lagier.

REFERENCES

ANAGNOSTOPOULOS, T. (1973). Biionic potentials in the proximal tubule of *Necturus* kidney. *Journal of Physiology* **233**, 375–394.

BOTT, P. A. (1962). Micropuncture study of renal excretion of water, K, Na, and Cl in *Necturus*. *American Journal of Physiology* **203**, 662–666.

CHAILLET, J. R., LOPES, A. G. & BORON, W. F. (1985). Basolateral Na–H exchange in the rabbit cortical collecting tubule. *Journal of General Physiology* **86**, 795–812.

COHEN, B., GIEBISCH, G., HANSEN, L. L., TEUSCHER, U. & WIEDERHOLT, M. (1984). Relationship between peritubular membrane potential and net fluid reabsorption in the distal renal tubule of *Amphiuma*. *Journal of Physiology* **348**, 115–134.

DURANTI, E., EHRENFELD, J. & HARVEY, B. J. (1986). Acid secretion through the *Rana esculenta* skin: involvement of an anion-exchange mechanism at the basolateral membrane. *Journal of Physiology* **378**, 195–211.

EDELMAN, A., BOUTHIER, M. & ANAGNOSTOPOULOS, T. (1981). Chloride distribution in the proximal convoluted tubule of *Necturus* kidney. *Journal of Membrane Biology* **62**, 7–17.

FISCHER, J. L., HUSTED, R. F. & STEINMETZ, P. R. (1983). Chloride dependence of the HCO_3^- exit step in urinary acidification in turtle bladder. *American Journal of Physiology* **245**, F564–568.

García-Díaz, J. F., Klemperer, G., Baxendale, L. M. & Essig, A. (1986). Cell sodium activity and sodium pump function in frog skin. *Journal of Membrane Biology* **92**, 37–46.

Garland, H. O., Henderson, I. W. & Brown, J. A. (1975). Micropuncture study of the renal responses of the urodele amphibian *Necturus* maculosus to injections of arginine vasotocin and an anti-aldosterone compound. *Journal of Experimental Biology* **63**, 249–264.

Gluck, S. & Al-Awqati, Q. (1984). An electrogenic proton-translocating adenosine triphosphatase from bovine kidney medulla. *Journal of Clinical Investigation* **73**, 1704–1710.

Halm, D. R. & Frizzell, R. A. (1986). Active K transport across rabbit distal colon: relation to Na absorption and Cl secretion. *American Journal of Physiology* **251**, C252–267.

Hanley, M. J., Kokko, J. P., Gross, J. B. & Jacobson, H. R. (1980). Electrophysiologic study of the cortical collecting tubule of the rabbit. *Kidney International* **17**, 74–81.

Hoshi, T., Suzuki, Y. & Itoi, K. (1981). Differences in functional properties between the early and late segments of the distal tubule of amphibian (*Triturus*) kidney. *Japanese Journal of Nephrology* **23**, 889–896.

Khuri, R. N., Agulian, S. K. & Bogharian, K. (1974). Electrochemical potentials of chloride in distal renal tubule of the rat. *American Journal of Physiology* **227**, 1352–1355.

Koeppen, B. M. & Helman, S. I. (1982). Acidification of luminal fluid by the rabbit cortical collecting tubule perfused *in vitro*. *American Journal of Physiology* **242**, F521–531.

Lee, C. O., Taylor, A. & Windhager, E. E. (1980). Cytosolic calcium ion activity in epithelial cells of *Necturus* kidney. *Nature* **287**, 859–861.

Nicol, S. C., Glass, M. L. & Heisler, N. (1983). Comparison of directly determined and calculated plasma bicarbonate concentration in the turtle *Chrysemis picta bellii* at different temperatures. *Journal of Experimental Biology* **107**, 521–525.

Persson, B. E. & Persson, A. E. G. (1983). Acidification of the distal tubule of *Amphiuma* kidney. *Acta physiologica scandinavica* **117**, 343–349.

Planelles, G., Kurkdjian, A. & Anagnostopoulos, T. (1984). Cell and luminal pH in the proximal tubule of *Necturus* kidney. *American Journal of Physiology* **247**, F932–938.

Planelles, G., Moreau, K. & Anagnostopoulos, T. (1983). Reinvestigation of the transepithelial p.d. in the proximal tubule of *Necturus* kidney. *Pflügers Archiv* **396**, 41–48.

Reeves, R. B. (1976). Temperature-induced changes in blood acid–base status: pH and P_{CO_2} in a binary buffer. *Journal of Applied Physiology* **40**, 752–761.

Ridderstråle, Y. (1976). Intracellular localization of carbonic anhydrase in the frog nephron. *Acta physiologica scandinavica* **98**, 465–469.

Robinson, R. A. & Stokes, R. H. (1959). *Electrolyte Solutions*. London: Butterworth.

Sachs, G., Chang, H., Rabon, E., Schackmann, R., Lewin, M. & Saccomani, G. (1976). A non-electrogenic H^+-pump in plasma membrane of hog stomach. *Journal of Biological Chemistry* **251**, 7690–7698.

Sansom, S. C., Weinman, E. J. & O'Neil, R. G. (1984). Microelectrode assessment of chloride-conductive properties of cortical collecting duct. *American Journal of Physiology* **247**, F291–302.

Spring, K. R. & Kimura, G. (1978). Chloride reabsorption by renal proximal tubule of *Necturus*. *Journal of Membrane Biology* **38**, 233–254.

Star, R. A., Burg, M. B. & Knepper, M. A. (1985). Bicarbonate secretion and chloride absorption by rabbit cortical collecting ducts. *Journal of Clinical Investigation* **76**, 1123–1130.

Stone, D. K., Seldin, D. W., Kokko, J. P. & Jacobson, H. R. (1983). Anion dependence of rabbit medullary collecting duct acidification. *Journal of Clinical Investigation* **71**, 1505–1508.

Stoner, L. C. (1977). Isolated, perfused amphibian renal tubules: the diluting segment. *American Journal of Physiology* **233**, F438–444.

Stoner, L. C., Burg, M. B. & Orloff, J. (1974). Ion transport in cortical collecting tubule: effect of amiloride. *American Journal of Physiology* **227**, 453–459.

Tago, K., Schuster, V. L. & Stokes, J. B. (1986). Stimulation of chloride transport by HCO_3–CO_2 in rabbit cortical collecting tubule. *American Journal of Physiology* **251**, F49–56.

Teulon, J. & Anagnostopoulos, T. (1982*a*). The electrical profile of the distal tubule in *Triturus* kidney. *Pflügers Archiv* **395**, 138–144.

Teulon, J. & Anagnostopoulos, T. (1982*b*). Proximal cell K^+ activity: Technical problems and dependence on plasma K^+ concentration. *American Journal of Physiology* **243**, F12–18.

Teulon, J., Froissart, P. & Anagnostopoulos, T. (1985). Electrochemical profile of K^+ and Na^+ in the amphibian early distal tubule. *American Journal of Physiology* **248**, F266–271.

VELÁZQUEZ, H. & WRIGHT, F. (1986). Effects of diuretic drugs on Na, Cl, and K transport by rat renal distal tubule. *American Journal of Physiology* **250**, F1013–1023.

WHITE, J. F. (1985). Omeprazole inhibits H^+ secretion by *Amphiuma* jejunum. *American Journal of Physiology* **248**, G256–259.

WIEDERHOLT, M., SULLIVAN, W. J. & GIEBISCH, G. (1971). Potassium and sodium across single distal tubules of *Amphiuma*. *Journal of General Physiology* **57**, 495–525.